Inorg. Chem. **2006**, *45*, 1201–1207

Systematic Synthesis and Characterization of Single-Crystal Lanthanide Phenylphosphonate Nanorods

Shu-Yan Song,[†] Jian-Fang Ma,*[,†] Jin Yang,[†] Min-Hua Cao,[†] Hong-Jie Zhang,[‡] Hai-Shui Wang,[‡] and Kui-Yue Yang[‡]

Department of Chemistry, Northeast Normal University, Changchun 130024, People's Republic of China, and Laboratory of Rare Earth Chemistry and Physics, Changchun Institute of Applied Chemistry, Chinese Academy of Sciences, Changchun 130022, People's Republic of China

Received October 10, 2005

Using low-temperature hydrothermal methods, nanoscale lanthanide phenylphosphonates species with different morphologies, namely, nanoparticles and nanorods, have been systematically synthesized. The possible growth mechanism of these nanorods was discussed. X-ray diffraction, transmission electron microscopy, electron diffraction, and photoluminescence spectra were used to characterize these materials. The photoluminescent properties of $Eu(O_3PC_6H_5)(HO_3PC_6H_5)$ and $La_{0.91}Eu_{0.09}(O_3PC_6H_5)(HO_3PC_6H_5)$ nanorods were discussed.

Introduction

Open-framework metallophosphonates with rich compositional and structure diversity have attracted considerable attention in recent years due to their potential applications in catalysis, ion exchange, proton conductivity, intercalation chemistry, and materials chemistry.[1] Most of the compounds studied are layered species in which the metal octahedra are bridged by phosphonic acid tetrahedra to form two-dimensional layers that are separated by the hydrophobic regions of the organic moieties.[2] Examples of their demonstrated applications include Langmuir−Blodgett and other types of thin films, nonlinear optical materials, proton conductors, sorbents, molecular sieves, and sensors.[3] Clearfield et al. have synthesized a series of phenylphosphonates of the lanthanide elements, some of which single crystals have been obtained and the crystal structures determined.[4] This kind of compound forms a relatively new class of alternating inorganic and organic layers and has received significant interest in recent years, as well established in excellent reviews.[5] Moreover, $Ln(O_3PC_6H_5)(HO_3PC_6H_5)$ compounds (Ln = Eu, Tb) have been extensively used as high-performance luminescent devices resulting from the 4f shell of their ions.[6] The properties of these inorganic and organic hybrid materials, such as catalytic activity, conductivity, or photonic efficiency, are often closely related to their chemical composition, size, crystal structure, surface chemistry, and shape.[7] Nanoscale materials can offer larger surface areas than the corresponding solid films or bulk materials; as a consequence, developing new method for the synthesis of nanosize lanthanide phosphonates, especially 1D nanorods, to tailor their electronic, magnetic, and optical properties proves to be intriguing and valuable.

1D nanomaterials represent a class of quasi-one-dimensional materials, in which carrier motion is restricted in two directions so that they usually exhibit significant photochemical, photophysical, and electron-transport properties that differ from those of bulk materials.[8,9] Many important materials have been prepared in the form of nanorods or

* To whom correspondence should be addressed. E-mail: jianfangma@yahoo.com.cn.
[†] Northeast Normal University.
[‡] Chinese Academy of Sciences.

(1) (a) Alberti, G. In *Comprehensive Supramolecular Chemistry*; Alberti, G., Bein, T., Eds.; Pergamon: London, 1996; Vol. 7, p 151. (b) Clearfield, A. *Chem. Mater.* **1998**, *10*, 2801. (c) Dines, M. B.; DiGiacomo, P. M. *Inorg. Chem.* **1981**, *20*, 92. (d) Cao, G.; Lee, H.; Lynch, V. M.; Mallouk, T. E. *Inorg. Chem.* **1988**, *27*, 2781. (e) Song, J. L.; Prosvirin, A. V.; Zhao, H. H.; Mao, J. G. *Eur. J. Inorg. Chem.* **2004**, 3706.
(2) (a) Finn, E.; Burkholder, R. C.; Zubieta, J. *Chem. Commun.* **2001**, 1852. (b) Finn, R. C.; Zubieta, J. *Inorg. Chem.* **2001**, *40*, 2466. (c) Mao, J. G.; Clearfield, A. *Inorg. Chem.* **2002**, *41*, 2319. (d) Zhu, J.; Bu, X.; Feng, P.; Stucky, G. D. *J. Am. Chem. Soc.* **2000**, *122*, 11563.
(3) (a) Cao, G.; Hong, H. G.; Mallouk, T. *Acc. Chem. Res.* **1992**, *25*, 420. (b) Thompso, M. *Chem. Mater.* **1994**, *6*, 1168.
(4) Wang, R. C.; Zhang, Y.; Hu, H.; Frausto, R. R.; Clearfield, A. *Chem. Mater.* **1992**, *4*, 864.
(5) (a) Clearfield, A. *Curr. Opin. Solid State Mater. Sci.* **1996**, *1*, 268. (b) Clearfield, A. *Curr. Opin. Solid State Mater. Sci.* **2002**, *6*, 495.
(6) (a) Rosa, I. L. V.; Nassar, E. J.; Serra, O. A. *J. Alloys Compd.* **1998**, *275*, 315. (b) Panigrahi, B. S. *Luminescence* **1999**, *82*, 121.
(7) (a) Zhu, Y.-C.; Bando, Y.; Xue, D.-F.; Golberg, D. *Adv. Mater.* **2004**, *16*, 831. (b) Bonchio, M.; Carraro, M.; Scorrano, G.; Bagno, A. *Adv. Synth. Catal.* **2004**, *346*, 648. (c) Johnson, C. J.; Edler, K. J.; Mann, S.; Murphy, C. J. *J. Mater. Chem.* **2002**, 2909.

10.1021/ic051749j CCC: $33.50
Published on Web 01/10/2006

nanowires to generate some unexpected properties based on which many new potential applications have been explored, such as well-controlled and monodisperse CdSe nanorods used in solar cell and well-defined ZnO nanowires that served as natural resonance cavities.[8b−d] Many methods have been used to prepare 1D nanomaterials, such as electrochemistry, templates (mesoporous silica, carbon nanotubes, etc.), emulsion or polymetric systems, arc discharge, and organometallic and coordination chemistry methods.[10] These methods often suffer from the requirements of high temperature, special conditions, tedious procedures, and catalysts or templates, which result in the difficulty with large-scale production. Low-temperature hydrothermal methods have been regarded as an effective route to fabrication of high-quality anisotropic nanomaterials.[11] Some studies have been reported on the synthesis and characterization of lanthanide phosphates nanowires and nanorods by hydrothermal processes.[12,13] In most of these studies, the formation of 1D nanosize $LnPO_4$ is due to their own anisotropic crystal structures and without any surfactants. Recently we have successfully synthesized nanosize transition metal phenylphosphonates, namely, nanorods and nanoparticles.[14] Herein, we report on a low-temperature hydrothermal method for the preparation of lanthanide phenylphosphonates $Ln(O_3PC_6H_5)(HO_3PC_6H_5)$ (Ln = La, Ce, Pr, Nd, Sm, Eu, Gd, Tb, Dy, Ho, Er, Tm, Yb, and Lu) nanorods.

Experimental Section

All chemical reagents were of analytical grade and used as received without further purification. $Ln(O_3PC_6H_5)(HO_3PC_6H_5)$ nanorods were prepared by a simple low-temperature hydrothermal method. In a typical procedure, 0.20 mmol of $LnCl_3$ with 0.14 g of sodium *p*-toluenesulfonate (STS) and 0.40 mmol of phenylphosphonic acid were dissolved in 5 mL of distilled water, respectively, and then were mixed and stirred for about 40 min. The pH was adjusted to 2.0 using NaOH aqueous solution. The resulting suspension was transferred into a stainless steel autoclave with a Teflon liner of 23 mL capacity and heated in an oven at 100 °C for 48 h. After the autoclave was air-cooled to room temperature unaided, the resulting precipitate was filtered out and washed with distilled water and absolute ethanol and finally dried under vacuum at 60 °C for 4 h.

X-ray power diffraction (XRD) patterns of the samples were collected on a Rigaku D_{max} 2000 X-ray diffractometer with Cu Kα radiation ($\lambda = 0.154\,178$ nm), 2θ ranging from 4 to 70°. TEM and HRTEM were recorded on a Hitachi model H-800 transmission electron microscope, using an accelerating voltage of 200 kV. Elemental analysis for rare earth was carried out by XRF analysis on a Shimadzu XRF-1700 sequential X-ray fluorescence spectrometer.

Result and Discussion

Synthesis and Characterization of $Ln(O_3PC_6H_5)(HO_3PC_6H_5)$ Nanorods. $Ln(O_3PC_6H_5)(HO_3PC_6H_5)$ nanorods were obtained by the reaction of $LnCl_3$ and phenlyphosphonic acid using hydrothermal method in the presence of sodium *p*-toluenesulfonate (STS), whereas $La(O_3PC_6H_5)(HO_3PC_6H_5)$ nanoparticles were obtained in the absence of STS.

$La(O_3PC_6H_5)(HO_3PC_6H_5)$ is triclinic with $Z = 2$, $a = 8.410(3)$ Å, $b = 15.696(7)$ Å, $c = 5.636(1)$ Å, $\alpha = 90.24(4)°$, $\beta = 108.99\ (1)°$, and $\gamma = 85.59(4)°$.[4] Figure 1 shows the XRD patterns of the samples, and the measurements indicate that these samples display a similar crystal structure. Both XRD patterns of nanorods (La) and nanoparticles (La1) of $La(O_3PC_6H_5)(HO_3PC_6H_5)$ can be well indexed to the simulated XRD powder pattern of $La(O_3PC_6H_5)(HO_3PC_6H_5)$ (Figure 2), indicating that they are the same compound. It can be seen from Figure 1 that the 2θ values of the XRD peaks gradually increase on going from $La(O_3PC_6H_5)(HO_3PC_6H_5)$ to $Lu(O_3PC_6H_5)(HO_3PC_6H_5)$, indicating the gradual shrinkage of lattice constants and cell volumes. This shrinkage of the lattice constants with atomic number is believed to be caused by the contraction of the ionic radii of Ln^{3+}. The ionic radii of Ln^{3+} and the *d* values of (010) are listed in Table 1.

(8) (a) Duan, X. F.; Huang, Y.; Cui, Y.; Wang, J. F.; Lieber, C. M. *Nature* **2001**, *409*, 66. (b) Huynh, W. U.; Dittmer, J. J.; Alivisatos, A. P. *Science* **2002**, *295*, 2425. (c) Li, L. S.; Walda, J.; Manna, L.; Alivisatos, A. P. *Nano Lett.* **2002**, *2*, 557. (d) Huang, M. H.; Mao, S.; Feick, H.; Yan, H. Q.; Wu, Y. Y.; Kind, H.; Weber, E.; Russo, R.; Yang, P. D. *Science* **2001**, *292*, 1897. (e) Law, M.; Kind, H.; Messer, B.; Kim, F.; Yang, P. D. *Angew. Chem., Int. Ed.* **2002**, *41*, 2405. (f) Ge, J. P.; Li, Y. D. *Chem. Commun.* **2003**, 2498.

(9) (a) Yu, W. W.; Peng, X. G. *Angew. Chem., Int. Ed.* **2002**, *41*, 2368. (b) Sun, Y. G.; Gates, B.; Mayers, B.; Xia, Y. N. *Nano Lett.* **2002**, *2*, 165. (c) Wang, X.; Li, Y. D. *J. Am. Chem. Soc.* **2002**, *124*, 2880. (d) Li, Y. D.; Wang, J. W.; Deng, Z. X.; Wu, Y. Y.; Sun, X. M.; Yu, D. P.; Yang, P. D. *J. Am. Chem. Soc.* **2001**, *123*, 9904. (e) Pan, Z. W.; Dai, Z. R.; Ma, C.; Wang, Z. L. *J. Am. Chem. Soc.* **2002**, *124*, 1817.

(10) (a) Wu, Y.; Yan, H.; Huang, M.; Messer, B.; Song, J. H.; Yang, P. *Chem.—Eur. J.* **2002**, *8*, 1261. (b) Routkevitch, D.; Bigioni, T.; Moskovits, M.; Xu. J. M. *J. Phys. Chem.* **1996**, *100*, 14037. (c) Han, W.; Fan, S.; Li, Q.; Hu, Y. *Science* **2002**, *296*, 884. (d) Rao, C. N. R.; Deepak, F. L.; Gundiah, G.; Govindaraj, A. *Prog. Solid State Chem.* **2003**, *31*, 5. (e) Ajayan, P. M.; Stephan, O.; Redlich, P.; Colliex, C. *Nature* **1995**, *375*, 564. (f) Xia, Y. N.; Yang, P. D.; Sun, Y.; Wu, Y.; Mayers, B.; Gates, B.; Yin, Y.; Kim, F.; Yan, H. *Adv. Mater.* **2003**, *15*, 353. (g) Peng, Z. A.; Peng, X. *J. Am. Chem. Soc.* **2002**, *124*, 3343. (h) Wang, X.; Li, Y. D. *Angew. Chem., Int. Ed.* **2002**, *41*, 4790.

(11) (a) Patzke, G. R.; Krumeich, F.; Nesper, R. *Angew. Chem., Int. Ed.* **2002**, *41*, 2446. (b) Cao, M.; Hu, C.; Wang, Y.; Guo, Y.; Guo, C.; Wang, E. *Chem. Commun.* **2003**, 1884. (c) Li, Y. D.; Li, X. L.; Deng, Z. X.; Zhou, B.; Fan, S.; Wang, J.; Sun, X. *Angew. Chem., Int. Ed.* **2002**, *41*, 333. (d) Rao, C. N. R.; Satishkumar, B. C.; Govindaraj, A. *Chem. Commun.* **1997**, 1581. (e) Peng, X. G.; Manna, L.; Yang, W. D.; Wickham, J.; Scher, E.; Kadavanich, A.; Alivisatos, A. P. *Nature* **2000**, *404*, 59. (f) Peng, Z. A.; Peng, X. *J. Am. Chem. Soc.* **2001**, *123*, 1389.

(12) (a) Riwotzki, K.; Meyssamy, H.; Schnablegger, H.; Kornowski, A.; Haase, M. *Angew. Chem., Int. Ed.* **2001**, *40*, 573. (b) Riwotzki, K.; Meyssamy, H.; Kornowski, A.; Haase, M. *J. Phys. Chem. B* **2000**, *104*, 2824. (c) Schuetz, P.; Caruso, F. *Chem. Mater.* **2002**, *14*, 4509. (d) Nishihama, S.; Hirai, T.; Komasawa, I. *J. Mater. Chem.* **2002**, *12*, 1053. (e) Heer, S.; Lehmann, O.; Haase, M.; Güdel, H. U. *Angew. Chem., Int. Ed.* **2003**, *42*, 3179. (f) Yan, R.; Sun, X.; Wang, X.; Peng, Q.; Li, Y. *Chem.—Eur. J.* **2005**, *11*, 2183. (g) Kong, X. Y.; Ding, Y.; Yang, R.; Wang, Z. L. *Science* **2004**, *303*, 1348. (h) Cao, M.; Hu, C.; Wang, E. *J. Am. Chem. Soc.* **2003**, *125*, 11196. (i) Cao, M.; Wu, X.; He, X.; Hu, C. *Chem. Commun.* **2005**, 2241.

(13) (a) Ito, H.; Fujishiro, Y.; Sato, T.; Okuwaki, A. *Br. Ceram. Trans.* **1995**, *94*, 146. (b) Meyssamy, H.; Riwotzki, K.; Kornowski, A.; Naused, S.; Haase, M. *Adv. Mater.* **1999**, *11*, 840. (c) Zhang, Y. J.; Guan, H. M. *J. Cryst. Growth* **2003**, *256*, 156. (d) Guan, H. M.; Zhang, Y. J. *J. Solid State Chem.* **2004**, *177*, 781. (e) Fang, Y. P.; Xu, A. W.; Song, R. Q.; Zhang, H. X.; You, L. P.; Yu, J. C.; Liu, H. Q. *J. Am. Chem. Soc.* **2003**, *125*, 16025. (f) Zhang, Y. W.; Yan, Z. G.; You, L. P.; Si, R.; Yan, C. H. *Eur. J. Inorg. Chem.* **2003**, 4099. (g) Yan, Z. G.; Zhang, Y. W.; You, L. P.; Si, R.; Yan, C. H. *J. Cryst. Growth* **2004**, *262*, 408.

(14) Song, S. Y.; Ma, J. F.; Yang, J.; Cao, M. H.; Li, K. C. *Inorg. Chem.* **2005**, *44*, 2140.

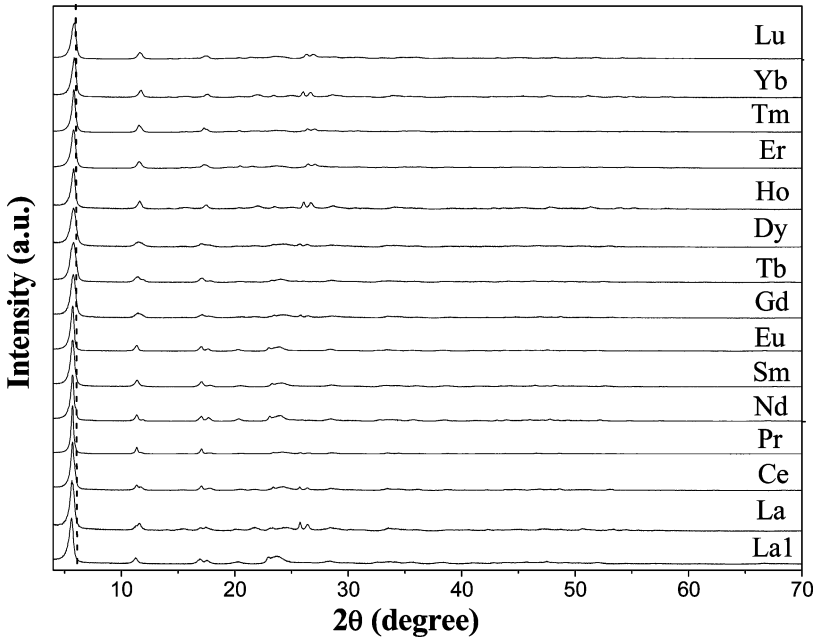

Figure 1. XRD patterns of $Ln(O_3PC_6H_5)(HO_3PC_6H_5)$ (La−Lu) nanorods and $La(O_3PC_6H_5)(HO_3PC_6H_5)$ nanoparticles (La1).

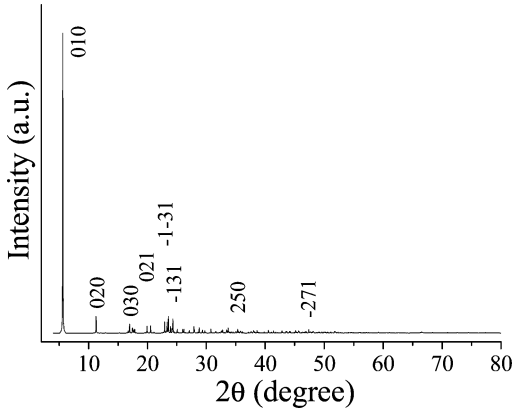

Figure 2. Simulated XRD powder pattern of $La(O_3PC_6H_5)(HO_3PC_6H_5)$.

The panoramic morphologies of obtained products were examined using TEM, in which the solid samples were mounted on a copper mesh with a dispersion treatment. The results indicate that the products consist of nanorods and a few nanoparticles. As shown in Figure 3b,c, typical TEM images show that sample La consists of rodlike shape with diameters of 40−60 nm and lengths of 100−500 nm and particlelike shape with diameters of 40−60 nm. More details about the structure of nanorods were investigated using high-resolution transmission electron microscopy (HRTEM) and

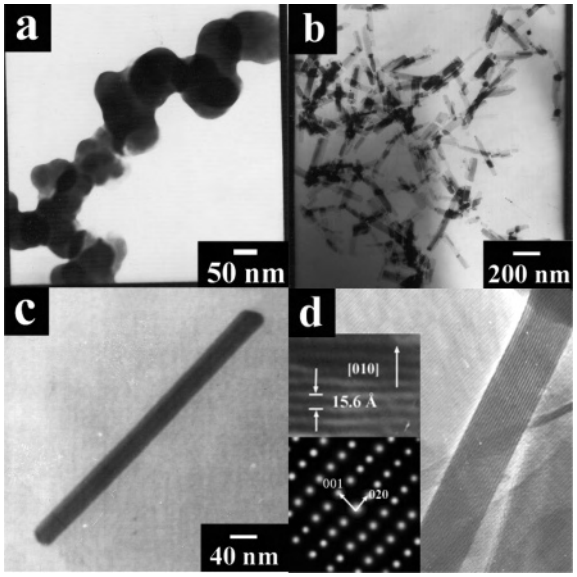

Figure 3. TEM images of $La(O_3PC_6H_5)(HO_3PC_6H_5)$: (a) nanoparticles; (b, c) nanorods; (d) HRTEM of $La(O_3PC_6H_5)(HO_3PC_6H_5)$ nanorod (inset is the SAED image).

the selected area electron diffraction (SAED). The HRTEM and SAED images (Figure 3d) of the nanorods show that the obtained rods are structurally uniform and monocrystalline, growing along the [002] direction. The TEM image of

Table 1. Effective Ionic Radii of Ln^{3+} and the *d* Values of (010)

param	Ln^{3+} / La^{3+}	Ce^{3+}	Pr^{3+}	Nd^{3+}	Sm^{3+}	Eu^{3+}	Gd^{3+}
ionic radius (Å)	116.0	114.3	112.6	110.9	107.9	106.6	105.3
d values of (010) (Å)	15.6015	15.4931	15.4926	15.4912	15.4388	15.4386	15.3304
param	Ln^{3+} / Tb^{3+}	Dy^{3+}	Ho^{3+}	Er^{3+}	Tm^{3+}	Yb^{3+}	Lu^{3+}
ionic radius (Å)	104.0	102.7	101.5	100.4	99.4	98.5	97.7
d values of (010) (Å)	15.2776	15.2773	15.2261	15.2257	15.1735	15.0695	15.0690

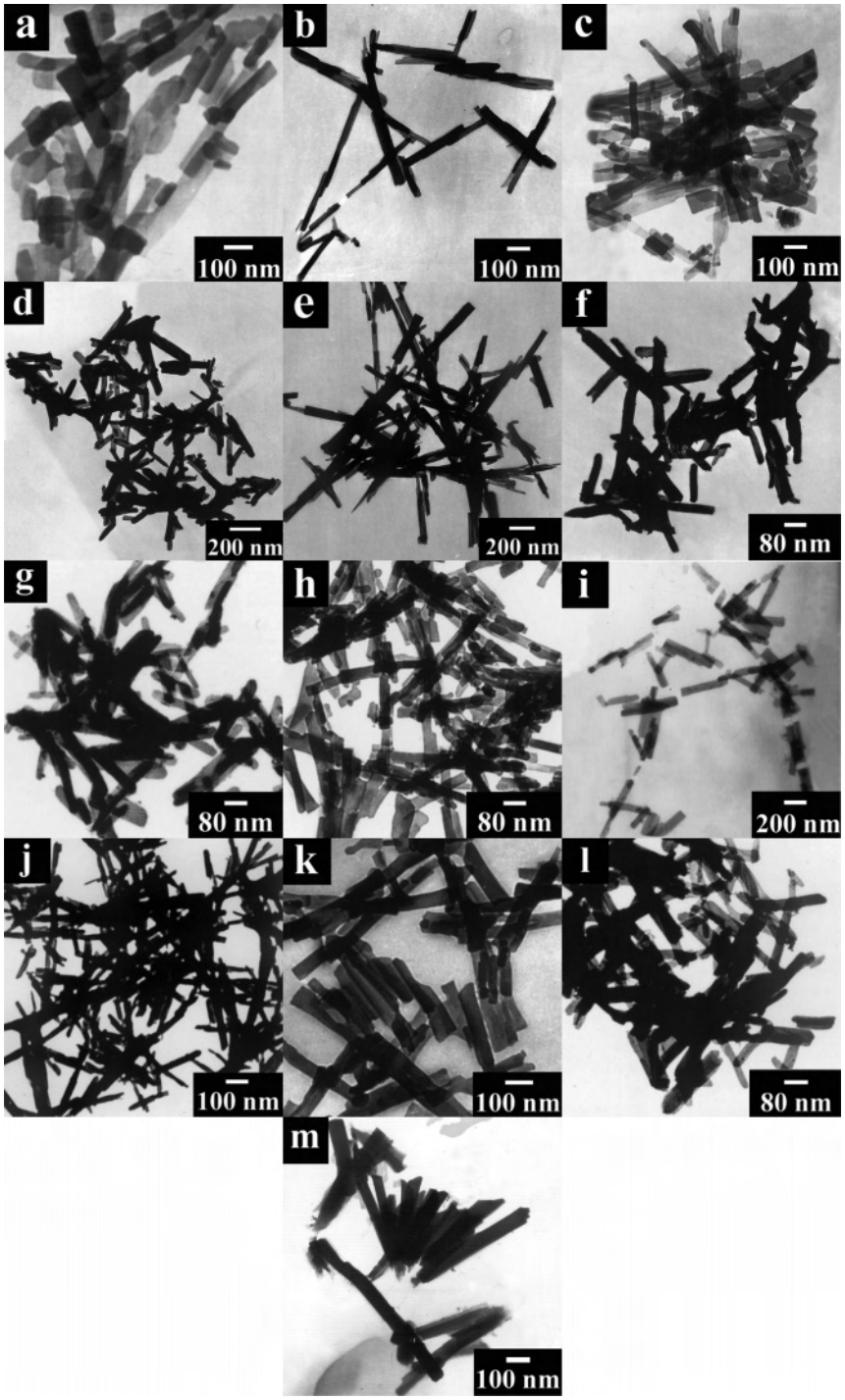

Figure 4. TEM images of $Ln(O_3PC_6H_5)(HO_3PC_6H_5)$ nanorods: Ln = Ce (a), Pr (b), Nd (c), Sm (d), Eu (e), Gd (f), Tb (g), Dy (h), Ho (i), Er (j), Tm (k), Yb (l), and Lu (m).

$La(O_3PC_6H_5)(HO_3PC_6H_5)$ nanoparticles is shown in Figure 3a. The TEM images of other $Ln(O_3PC_6H_5)(HO_3PC_6H_5)$ (Ln = Ce, Pr, Nd, Sm, Eu, Gd, Tb, Dy, Ho, Er, Tm, Yb, and Lu) nanorods are shown in Figure 4.

Eu^{3+}-doped $La(O_3PC_6H_5)(HO_3PC_6H_5)$ nanorods were prepared by the same hydrothermal treatment as the undoped sample, and in this work the original concentration of dopant Eu^{3+} ions is 10 mol %. Anal. Found: La, 27.90; Eu, 3.02. So the product can be expressed as $La_{0.91}Eu_{0.09}(O_3PC_6H_5)(HO_3PC_6H_5)$. The TEM image of the obtained $La_{0.91}Eu_{0.09}(O_3PC_6H_5)(HO_3PC_6H_5)$ product was shown in Figure 5, and it

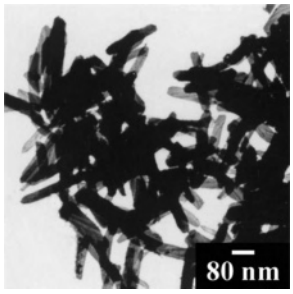

Figure 5. TEM images of the $La_{0.91}Eu_{0.09}(O_3PC_6H_5)(HO_3PC_6H_5)$ nanorod.

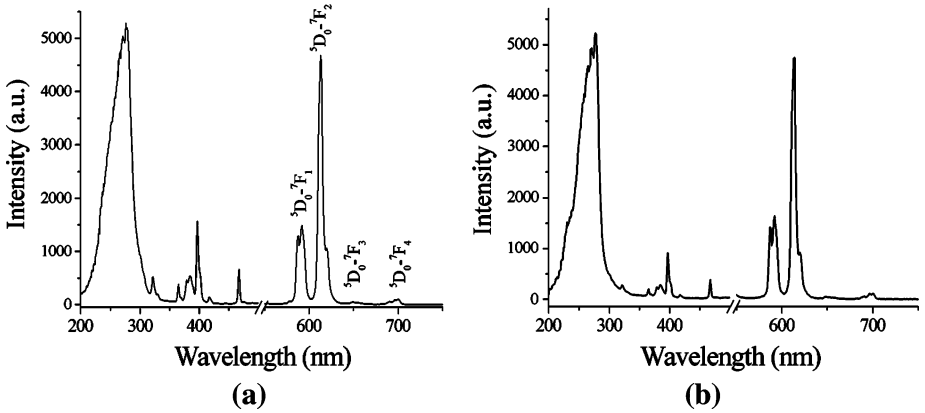

Figure 6. Luminescent spectra of bulk $Eu(O_3PC_6H_5)(HO_3PC_6H_5)$ (a) and $Eu(O_3PC_6H_5)(HO_3PC_6H_5)$ nanorods (b).

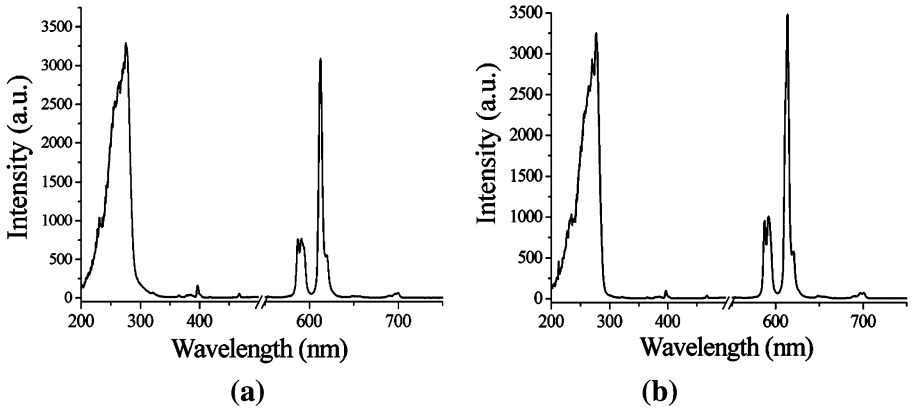

Figure 7. Luminescent spectra of Eu^{3+}-doped $La(O_3PC_6H_5)(HO_3PC_6H_5)$ bulk material (a) and nanorods (b).

can be seen that the samples maintain the morphology of the host material.

Photoluminescence of $Eu(O_3PC_6H_5)(HO_3PC_6H_5)$ and $La_{0.91}Eu_{0.09}(O_3PC_6H_5)(HO_3PC_6H_5)$ Nanorods. The luminescent spectra of bulk $Eu(O_3PC_6H_5)(HO_3PC_6H_5)$ and $Eu(O_3PC_6H_5)(HO_3PC_6H_5)$ nanorods are shown in Figure 6. The excitation spectra are recorded by monitoring the emission wavelength $\lambda_{em} = 615$ nm. The broad band with a maximum at 277 nm in the excitation spectrum of nanorods could be ascribed to the oxygen-to-europium charge-transfer band (CTB), which occurs by electron delocalization from the filled 2p shell of the O^{2-} to the partially filled 4f shell of Eu^{3+}. The CTB of bulk $Eu(O_3PC_6H_5)(HO_3PC_6H_5)$ is slightly broader than that of the nanorods, and the CTB peak position of the bulk sample (276 nm) is almost the same as that of nanorods. According to Li's work[12f] and previous studies,[15] the peak position of CTB is related to the length of the Eu−O bond; the longer the Eu−O bond is, the longer the wavelength of the CTB position will be. That means that the average Eu−O bond distance in $Eu(O_3PC_6H_5)(HO_3PC_6H_5)$ nanorods is almost the same as that of the bulk sample. The f−f transitions of the Eu^{3+} $4f^6$ electron configuration in the range of 300−500 nm can also be observed. These peaks are attributed to the direct excitation of the Eu^{3+} ground state into the higher levels of the 4f-manifold such as $^7F_0-^5L_6$ at 397 nm. The intensities of f−f transitions of the bulk sample are obviously higher than those of the nanorods. The emission spectrum of the nanorods is almost the same as that of the bulk sample, and the emission intensities for these two samples are almost the same. The electronic-dipole transition $^5D_0-^7F_2$ (613 nm) characterized by red emission is the most prominent component.

Since $Ln(O_3PC_6H_5)(HO_3PC_6H_5)$ (Ln = La, Gd and Lu) are transparent in the visible region, they can serve as host materials for other lanthanide ions to produce phosphors emitting different colors. The fluorescent studies of lanthanide-doped $Ln(O_3PC_6H_5)(HO_3PC_6H_5)$ have not been reported. In this study, Eu^{3+} ion was selected as a doping ions, and the fluorescence of Eu^{3+}-doped $La_{0.91}Eu_{0.09}(O_3PC_6H_5)(HO_3PC_6H_5)$ nanorods was studied.

The luminescent spectra of Eu^{3+}-doped bulk sample and nanorods of $La_{0.91}Eu_{0.09}(O_3PC_6H_5)$ $(HO_3PC_6H_5)$ are shown in Figure 7. The excitation spectra were recorded by monitoring the emission wavelength $\lambda_{em} = 615$ nm, and the emission spectra were recorded with the excitation wavelength $\lambda_{ex} = 277$ nm. The bulk sample and nanorods of $La_{0.91}Eu_{0.09}(O_3PC_6H_5)(HO_3PC_6H_5)$ show the same excitation and emission spectra, indicating that Eu^{3+} ions have been successfully doped into host $La(O_3PC_6H_5)(HO_3PC_6H_5)$ nanorods. Since $La(O_3PC_6H_5)(HO_3PC_6H_5)$ and $Eu(O_3PC_6H_5)(HO_3PC_6H_5)$ have similar crystal structures, the environment of the Eu^{3+} ion in $La_{0.91}Eu_{0.09}(O_3PC_6H_5)(HO_3PC_6H_5)$ nanorods is the same as that in $Eu(O_3PC_6H_5)(HO_3PC_6H_5)$ nanorods,

(15) (a) Wei, Z.; Sun, L.; Liao, C.; Yin, J.; Jiang, X.; Yan, C. *J. Phys. Chem. B* **2002**, *106*, 10610. (b) Hoefdraad, H. E. *J. Solid State Chem.* **1975**, *15*, 175. (c) Tao, Y.; Zhao. G.; Ju, X.; Shao, X.; Zhang, W.; Xia, S. *Mater. Lett.* **1996**, *28*, 17.

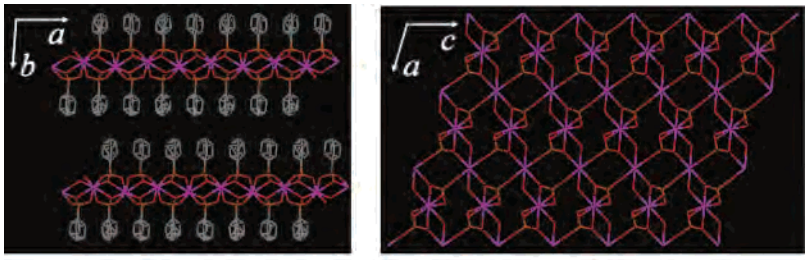

Figure 8. View of the structure of $La(O_3PC_6H_5)(HO_3PC_6H_5)$ along the *c* axis (a) and along the *b* axis (b).

and the emission spectrum of $La_{0.91}Eu_{0.09}(O_3PC_6H_5)(HO_3PC_6H_5)$ nanorods is almost the same as that of $Eu(O_3PC_6H_5)(HO_3PC_6H_5)$ nanorods. The emission intensity of the nanorods is a little bit higher than that of the bulk sample. The intensities of the Eu^{3+} ion f−f transitions in the range of 300−500 nm of $La_{0.91}Eu_{0.09}(O_3PC_6H_5)(HO_3PC_6H_5)$ nanorods are much lower than those of $Eu(O_3PC_6H_5)(HO_3PC_6H_5)$ nanorods because the concentration of Eu^{3+} in $La_{0.91}Eu_{0.09}(O_3PC_6H_5)(HO_3PC_6H_5)$ nanorods is lower than that of $Eu(O_3PC_6H_5)(HO_3PC_6H_5)$ nanorods.

Unlike other nanocrystals showing unique absorption and fluorescence characteristics such as CdSe and ZnO due to quantum size effects,[16] since the luminescence of both nanorods and bulk samples of $Eu(O_3PC_6H_5)(HO_3PC_6H_5)$ or $La_{0.91}Eu_{0.09}(O_3PC_6H_5)(HO_3PC_6H_5)$ originates from the f−f transitions of 4f shells which are well-shielded by the 5s and 5p shells of Eu^{3+} ions and the transitions of the f electrons are mainly affected by the local symmetry of the crystal site, size effects on the luminescence of $Eu(O_3PC_6H_5)(HO_3PC_6H_5)$ and $La_{0.91}Eu_{0.09}(O_3PC_6H_5)(HO_3PC_6H_5)$ nanorods are expected to be weak.[13e]

Possible Growth Mechanism of $Ln(O_3PC_6H_5)(HO_3PC_6H_5)$ Nanorods. As shown in Figure 8, $La(O_3PC_6H_5)(HO_3PC_6H_5)$ has a layered structure containing inorganic polymeric La−PO_3 layers attached by organic phenyl groups from both sides. The layers stack along the *b* axis to form a lamellar structure, and the structural feature along the *b* axis is greatly different from that along each of the *a* and *c* axes. A closer examination of the inorganic polymeric La−PO_3 layer suggested that the structural feature along the *c* axis is also different from that along the *a* axis although this difference is smaller than that between the structural features along the *b* and *c* or *a* axes. As shown in Figure 8b, each $PhPO_3^{2-}$ anion binds to La^{3+} ions of three adjacent La^{3+} layers which are parallel to (001) layers, whereas each $PhPO_3^{2-}$ anion binds to La^{3+} ions of two adjacent La^{3+} layers which are parallel to (100) layers. So the anisotropic characteristic along the *c* axis is different from that along the *a* axis. The anisotropic structural feature of $La(O_3PC_6H_5)(HO_3PC_6H_5)$ provides the base for the anisotropic growth of the nanocrystal. From a kinetic perspective, the activation energy for the [001] direction of growth of $La(O_3PC_6H_5)(HO_3PC_6H_5)$ is lower than that of growth along the *a* and *b* axes.[13e,17] This means a higher growth rate along the *c* axis and a lower one along the *a* and *b* axes to form $La(O_3PC_6H_5)(HO_3PC_6H_5)$ nanorods that grow preferentially along the [001] direction.

The experimental results indicate that STS plays a very important role in the growth of lanthanide phenylphosphonate nanorods. It is very difficult to give an exact thermodynamic prediction of the nanocrystal growth for this system. The role of STS may be explained by the formation of the loose complex through the electrostatic action between La^{3+} cation and *p*-toluenesulfonate anions. Peng et al. presented a three-stage shape evolution mechanism based on the spherical diffusion-controlled crystal growth theory.[10g] According to this mechanism, one-dimensional growth only occurs if the chemical potential of the monomers in solution is much higher than the highest chemical potential of the atom on the surface of the crystal seeds. In the absence of STS, the direct mixing of an aqueous solution of $LnCl_3$ and phenylphosphonic acid at pH = 2.0 leads to the formation of a large number of amorphous fine particles of the product. Small crystalline nuclei are formed under hydrothermal conditions, and the crystalline nanoparticles were obtained by transferring La^{3+} cations and phenylphosphonate anions from the smaller crystalline particles to the larger ones according to the well-known Gibbs−Thompson law. In the presence of high concentration of STS, the La^{3+} cations exist as complexes with *p*-toluenesulfonate anions. When phenylphosphonate was added, fine particles of the product were also formed. However, in this case the concentration of the La^{3+} complex with *p*-toluenesulfonate anions in the solution is higher than the concentration of the aqueous La^{3+} cation in the absence of STS. Thus, in the crystal growth stage, both monomers have high chemical potential, and this provides more favorable conditions for the growth of nanorods. Moreover, the addition of STS can significantly decrease the viscosity of the solution, which increases the mobility of the components in the system and allows atoms, ions, or molecules to adopt appropriate positions in developing crystal lattices.[18]

Li's report on the hydrothermal synthesis of CdE (E = S, Se, Te) nanorods in ethylenediamine provided a mechanism

(16) (a) Tang, Z.; Kotov, N. A.; Giersig, M. *Science* **2002**, *297*, 237. (b) Guo, L.; Ji, Y.; Xu, H.; Simon, P.; Wu, Z. *J. Am. Chem. Soc.* **2002**, *124*, 14864.

(17) Murphy, K. E.; Altman, M. B.; Wunderlich, B. *J. Appl. Phys.* **1977**, *48*, 4122.

(18) (a) Trentler, J. W.; Hickman, S. C.; Viano, A. M.; Gibbons, P. C.; Buhro, W. E. *Science* **1995**, *270*, 1791. (b) Tang, B.; Zhuo, L.; Ge, J.; Niu, J.; Shi, Z. *Inorg. Chem.* **2005**, *44*, 2568.

Scheme 1. Growth Mechanism of $La(O_3PC_6H_5)(HO_3PC_6H_5)$ Nanorods

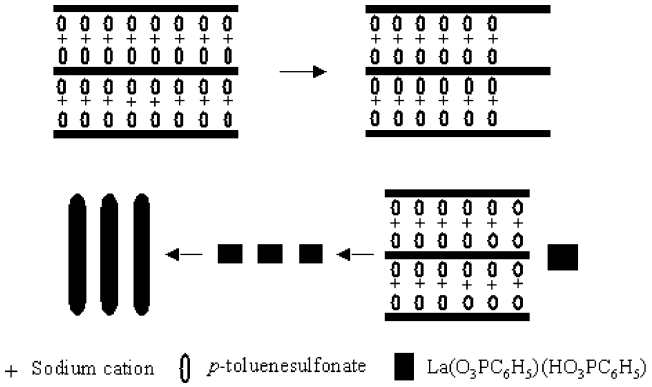

through a intermediate lamellar precursor.[19] Since $La(O_3PC_6H_5)(HO_3PC_6H_5)$ has a layered structure, Li's mechanism can also be applicable to the synthesis of $La(O_3PC_6H_5)(HO_3PC_6H_5)$ nanorods. As shown in Scheme 1, at the beginning of the synthesis, a lamellar precursor in which the layered structure of $La(O_3PC_6H_5)(HO_3PC_6H_5)$ is intercalated by STS was formed. During the hydrothermal treatments, the STS was removed, and the layered structure would crack into interlinked nanorods of $La(O_3PC_6H_5)(HO_3PC_6H_5)$.

(19) Deng, Z. X.; Li L.; Li, Y. *Inorg. Chem.* **2003**, *42*, 2331.

Conclusion

In summary, a low-temperature hydrothermal method was developed for the synthesis of lanthanide phenylphosphonate nanorods that are expected to exhibit some novel properties. The mechanism of synthesis and shape control of lanthanide phenylphosphonates is proposed from a kinetic perspective. This research includes a study of photoluminescence in $Eu(O_3PC_6H_5)(HO_3PC_6H_5)$ and Eu^{3+}-doped $La(O_3PC_6H_5)(HO_3PC_6H_5)$. The luminescent properties of these nanophosphors may lead to new and important opportunities in lanthanide chemistry.

Acknowledgment. We thank the National Natural Science Foundation of China (Grant No. 20471014), the Fok Ying Tung Education Foundation, the Laboratory of Rare Earth Chemistry and Physics in Changchun Institute of Applied Chemistry, and the Natural Science Foundation of Jilin province (China) for support. TEM work was performed by Dr. L.-H. Ge in Changchun Institute of Applied Chemistry, Chinese Academy of Sciences. Crystal data for $La(O_3PC_6H_5)(HO_3PC_6H_5)$ were obtained from Prof. A. Clearfield.

IC051749J